TISSUE ENGINEERING: Part A
Volume 16, Number 5, 2010

DOI: 10.1089/ten.tea.2009.0650

Inkjet-Based Biopatterning of Bone Morphogenetic Protein-2 to Spatially Control Calvarial Bone Formation

Gregory M. Cooper, Ph.D.,[1–3,*] Eric D. Miller, Ph.D.,[4,*] Gary E. DeCesare, M.D.,[1] Arvydas Usas, M.D.,[5] Emily L. Lensie, B.A.,[1] Michael R. Bykowski, M.S.,[1] Johnny Huard, Ph.D.,[3,5] Lee E. Weiss, Ph.D.,[6] Joseph E. Losee, M.D.,[1] and Phil G. Campbell, Ph.D.[4]

The purpose of this study was to demonstrate spatial control of osteoblast differentiation *in vitro* and bone formation *in vivo* using inkjet bioprinting technology and to create three-dimensional persistent bio-ink patterns of bone morphogenetic protein-2 (BMP-2) and its modifiers immobilized within microporous scaffolds. Semicircular patterns of BMP-2 were printed within circular DermaMatrix™ human allograft scaffold constructs. The contralateral halves of the constructs were unprinted or printed with BMP-2 modifiers, including the BMP-2 inhibitor, noggin. Printed bio-ink pattern retention was validated using fluorescent or ^{125}I-labeled bio-inks. Mouse C2C12 progenitor cells cultured on patterned constructs differentiated in a dose-dependent fashion toward an osteoblastic fate in register to BMP-2 patterns. The fidelity of spatial restriction of osteoblastic differentiation at the boundary between neighboring BMP-2 and noggin patterns improved in comparison with patterns without noggin. Acellular DermaMatrix constructs similarly patterned with BMP-2 and noggin were then implanted into a mouse calvarial defect model. Patterns of bone formation *in vivo* were comparable with patterned responses of osteoblastic differentiation *in vitro*. These results demonstrate that three-dimensional biopatterning of a growth factor and growth factor modifier within a construct can direct cell differentiation *in vitro* and tissue formation *in vivo* in register to printed patterns.

Introduction

Spatial patterning of cell function occurs during embryogenesis and throughout development.[1–6] Wound healing can be considered in part a recapitulation of embryogenesis. It involves complex spatial and temporal signaling interactions that direct all cell behaviors, including differentiation.[7–13] Biological patterning involves the creation of persistent patterns of a broad array of growth factors and their modifying molecules, leading to functional organization of multiple tissue types and organs. Extracellular matrix (ECM) molecules such as proteoglycans can sequester growth factors within the surrounding ECM or on the cell surface to modify growth factor function either negatively or positively.[14] Growth factor sequestration directly affects temporal and spatial function by presenting growth factors at specific locations in the ECM or on the cell surface[15–21] at picomolar to nanomolar concentrations.[22–26]

We previously demonstrated the application of inkjet-based biopatterning to print bio-inks of dilute aqueous solutions of native growth factors onto native ECM substrates to make persistent two-dimensional (2D) patterns.[27–31] In this context, the term 2D means surface patterning limited to printing bio-inks onto thin substrates of ECM films, such as a 10-nm-thick layer of fibrin crosslinked to glass slides. The growth factors were immobilized to the ECM substrates by taking advantage of the inherent native binding capacities between growth factors and ECM components.[32,33] These patterns were then used to direct cell fates *in vitro*, including migration, proliferation, and differentiation, in register to printed patterns.[27–31,34]

The question remained whether such growth factor patterning could translate into *in vivo* applications where

[1]Division of Plastic Surgery, Department of Surgery, University of Pittsburgh, Pittsburgh, Pennsylvania.
Departments of [2]Oral Biology, [3]Bioengineering, University of Pittsburgh, Pittsburgh, Pennsylvania.
[4]Institute of Complex Engineered Systems and Molecular Biosensor and Imaging Center and Departments of Biomedical Engineering, Materials Science and Engineering, and Biology, Carnegie Mellon University, Pittsburgh, Pennsylvania.
[5]Stem Cell Research Center, University of Pittsburgh, Pittsburgh, Pennsylvania.
[6]Robotic Institute, Carnegie Mellon University, Pittsburgh, Pennsylvania.
*These two authors contributed equally to this work.

three-dimensional (3D) constructs and patterns are required. To investigate this, we adapted our 2D biopatterning methodology to make 3D patterned constructs. Bio-inks were printed onto a sheet of porous scaffold material whereby they absorbed into and bound to the scaffold to form 3D patterned constructs. The primary requirements for 3D printing substrate materials are (1) open porosity and hydrophilicity for absorbing and internalizing a surface-applied bio-ink; (2) innate binding capacity for a broad range of growth factors and their modifiers; and (3) appropriate physical characteristics making them easy to handle during application. In addition, for use in investigations focusing on the role of growth factors in driving differentiation, these materials should possess relatively "neutral" material properties that do not have strong inherent stimulation capacity for any specific tissue type. It is important to emphasize that many surgically created wound sites do not require the use of scaffold materials that possess the same biomechanical properties as the targeted tissue to be regenerated because the scaffold is meant to be completely remodeled. DermaMatrix™ (Synthes, West Chester, PA) acellular dermal matrix fulfilled all these requirements. DermaMatrix is a human allograft material that maintains original dermal ECM architecture. It contains a range of ECM molecules, including collagens I and III, elastin, fibronectin, glycosaminoglycans, and proteoglycans, many of which can sequester or bind a broad range of growth factors and their modifiers.

This article presents the adaptation of our 2D bioprinting methodology to create persistent 3D spatial patterns of growth factors and their modifiers in a delivery scaffold. The bioprinting approach was demonstrated using printed bone morphogenetic protein-2 (BMP-2)/DermaMatrix constructs to spatially direct and restrict cellular differentiation down the osteogenic lineage *in vitro* and bone formation *in vivo* in a mouse calvarial defect model. Patterns of noggin, an inhibitor of BMP-2,[35] were also printed adjacent to the BMP-2 patterns to investigate fine control over patterned response discrimination. The fidelity of spatial restriction of osteoblastic differentiation *in vitro* and bone formation *in vivo* between neighboring BMP-2 and noggin patterns improved in comparison with patterns without noggin. Importantly, osteoinductive responses to BMP were achieved with substantially lower doses than generally reported.

Materials and Methods

In vitro—*biopatterning*

Bio-inks were printed using our custom 2D inkjet deposition system that was described in detail previously.[27] A drop-on-demand piezoelectric inkjet printhead with a 30-μm-diameter orifice (MicroFab Technologies, Plano, TX) was used for all growth factor patterning. The center-to-center drop spacing was set to 75 μm. To passivate the glass surface of the inkjet, it was filled with 1 μg/mL BSA (Sigma Chemical, St. Louis, MO) and incubated for 10 min. The jet was rinsed three times with deionized water and filled immediately with the bio-ink. The bio-inks consisted of human recombinant BMP-2, noggin, growth and differentiation factor-5 (GDF-5), and transforming growth factor-β1 (TGF-β1) (R&D Systems, Minneapolis, MN), each diluted in 10 mM sodium phosphate, pH 7.4, to final concentrations of 50, 100, or 200 μg/mL.

In vitro dosing studies consisted of printing an array of BMP-2 in varying concentrations as 1 mm×1 mm squares spaced 1 mm apart on a 10 mm×10 mm piece of ultrathin (200–400 μm thick) DermaMatrix™ derived from human acellular dermis (gift from Synthes). The bio-ink concentrations were held constant at 50, 100, or 200 μg/mL and surface concentration was controlled by varying the number of overprints (OPs),[27,31,34] including 2, 12, 22, and 32 OPs. Gradient patterns of Cy5-BMP-2 on DermaMatrix were also printed to

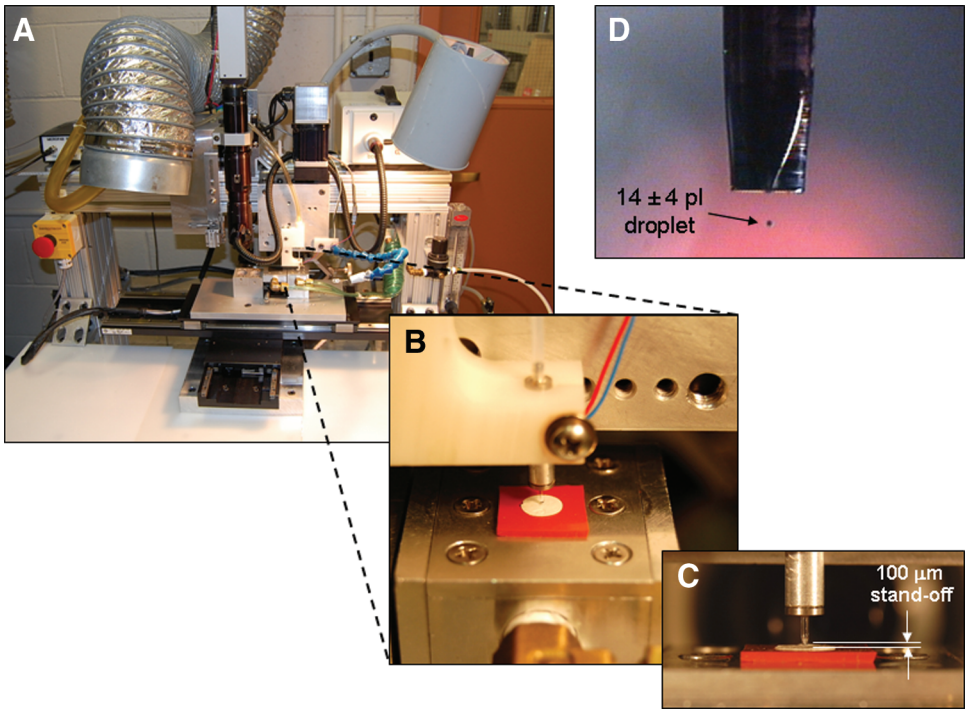

FIG. 1. Custom inkjet printing system (**A**) used to create three-dimensional printed constructs within DermaMatrix. (**B, C**) Growth factor bioink droplets averaged 14 pl (**D**). Color images available online at www.liebertonline.com/ten.

demonstrate the use of overprinting to modulate deposited concentration. Printed gradients were 1.5 mm long and 1 mm wide, with 80 μm spacing of deposited drops.

For the single-dose patterns used in all other experiments, bio-ink concentration was varied while maintaining a fixed number of 12 OPs. Patterns of BMP-2, noggin, GDF-5, and TGF-β1 were printed on DermaMatrix cut into 5-mm-diameter disks using 5 mm biopsy punches (MedExSupply Medical Supplies, Monsey, NY). A small notch was cut into one side of the DermaMatrix for registration purposes and the printing was performed on the dermal side of the scaffold. A semicircular pattern of BMP-2 was printed on one half of the construct; the other contralateral half was left unprinted or printed with noggin, GDF-5, or TGF-β1. For *in vivo* experiments, nonprinted (NP) DermaMatrix disks were used as additional controls. The printing setup used for these experiments is shown in Figure 1. The DermaMatrix was placed on the printing stages and was held in place during printing using a vacuum chuck.

Pattern validation and persistence

Fluorescently labeled BMP-2 was utilized to validate pattern printing on DermaMatrix. Fluorescent labeling of BMP-2 was performed as described previously.[34] Briefly, BMP-2 was labeled with monoreactive *N*-hydroxysuccinimide ester cyanine 5 dye (Cy5, synthesized in-house) following established protocols.[36] The Cy5-BMP-2 bio-inks were diluted in 10 mM sodium phosphate, pH 7.4, to the desired concentrations.

Patterns of the Cy5-BMP-2 were printed in the same manner as previously described.[31,34] For fluorescent-labeled BMP-2 printed gradients, 120 μg/mL Cy5-BMP-2 bio-ink was used. After printing, the constructs were imaged using a Zeiss Axioplan 2 epifluorescence microscope with a Fluor 2.5×, 0.12 numerical aperature (NA) objective, AxioCam MRm CCD camera, and AxioVision acquisition software v. 4.3 (all microscope components and software from Carl Zeiss, Thornwood, NY). The patterned constructs were then placed in phosphate-buffered saline (PBS) for approximately 30 min and imaged again.

Radiolabeling was used to quantify the binding and desorption of BMP-2 and noggin to determine the persistence of these applied bio-inks over time. BMP-2 and noggin were iodinated using a chloramine T method as described previously.[34,37] The concentrations of the ^{125}I-BMP-2 and ^{125}I-noggin were selected so that the surface concentrations prepared using the blotting would be comparable to what was inkjet printed. DermaMatrix samples were patterned by placing 1 μL of the prepared bio-ink onto the DermaMatrix substrate and allowing it to dry. After determining the quantity of ^{125}I-labeled BMP-2 or ^{125}I-noggin applied to each DermaMatrix sample using a Cobra II auto-gamma counter (Perkin-Elmer, Wellesley, MA), the slides were rinsed three times in PBS and the amount of ^{125}I-labeled components retained was determined again. The DermaMatrix samples were then placed in serum-free minimum essential alpha medium (α-MEM) with 25 mM HEPES, 0.02% sodium azide, and 1% penicillin/streptomycin and stored at 37°C for 24 h. The radioactive counts were determined again and the serum-free medium was replaced with serum-containing medium. The ^{125}I-BMP-2 and ^{125}I-noggin DermaMatrix samples were incubated in α-MEM containing 10% calf serum, the typical serum concentration used for *in vitro* experiments and to account for the likelihood that serum constituents may impact bio-ink binding retention. All acquired data were corrected to account for radioactive decay.

Determination of osteoblast differentiation in vitro

Osteoblast differentiation was assessed via alkaline phosphatase (ALP) in register to applied patterns of bio-inks. After patterning the disks of DermaMatrix, the constructs were secured to the bottom of the wells of a 24-well plate using sterile silicone grease, 1 mL of PBS was added to each construct, and the construct were placed in the incubator at 37°C overnight. The constructs were then rinsed with 1 mL of PBS and seeded with cells. C2C12 myogenic precursor cells were obtained from American Type Culture Collection (Manassas, VA) and cultured according to the American Type Culture Collection instructions in growth medium (Dulbecco's modified Eagle's medium [high-glucose], with 10% calf serum and 1% penicillin/streptomycin; Invitrogen, Carlsbad, CA). Each well was seeded with 200,000 cells in growth medium and placed in a standard incubator (5% CO_2, 37°C) for 48 h. After this culture period, the cells were rinsed in PBS and stained for ALP activity using a leukocyte ALP kit (product number 86C from Sigma Chemical) according to the manufacturer's instructions.

In vivo—*calvarial defects and bone healing analysis*

Sixty-eight normal male mice (C57BL-6J; Jackson, Bar Harbor, ME), 8 weeks of age, were used in this study. DermaMatrix disks were prepared as described earlier with BMP-2 on one half of the scaffold while the other half was untreated ($n = 10$) or printed with noggin ($n = 8$), and the constructs were placed in a 24-well plate with 1 mL of PBS and kept in the incubator at 37°C until implantation, which was within 2–4 days of the initial printing. Two separate control groups consisted of 10 animals in which the defect was left empty and 5 animals in which the defect was filled with unprinted DermaMatrix disks. These groups served to evaluate baseline healing inherent to the defect or to the osteogenic properties of the unprinted DermaMatrix.

The mice were anesthetized and the scalp depilated and cleaned prior to surgery. Under sterile conditions, a 5 mm circular bone defect was made in the skull using a 5.0 mm trephine (Fine Science Tools, Foster City, CA). One construct was placed within each skull defect with the orientation of the construct determined and assured using the notch that was cut in the DermaMatrix disk opposite to the BMP-2-printed side. Bone healing was assessed in representative animals using microcomputed tomography (VivaCT40; Scanco Medical, Easton, PA) analysis at 1 day, and 2, 4, and 8 weeks after surgery. After 4 or 8 weeks, animals were euthanized and the skulls removed and fixed in 10% neutral buffered formalin for subsequent analyses.

Traditional 2D radiographic images were collected from all fixed skulls using a Faxitron (MX-20; Faxitron X-Ray Corporation, Wheeling, IL), digitized, and measured with Northern Eclipse software (Empix Imaging, Cheektowaga, NY) to determine the remaining defect area. Photographs were taken of each skull to assess the final placement of the construct through identification of the notched side. Based on

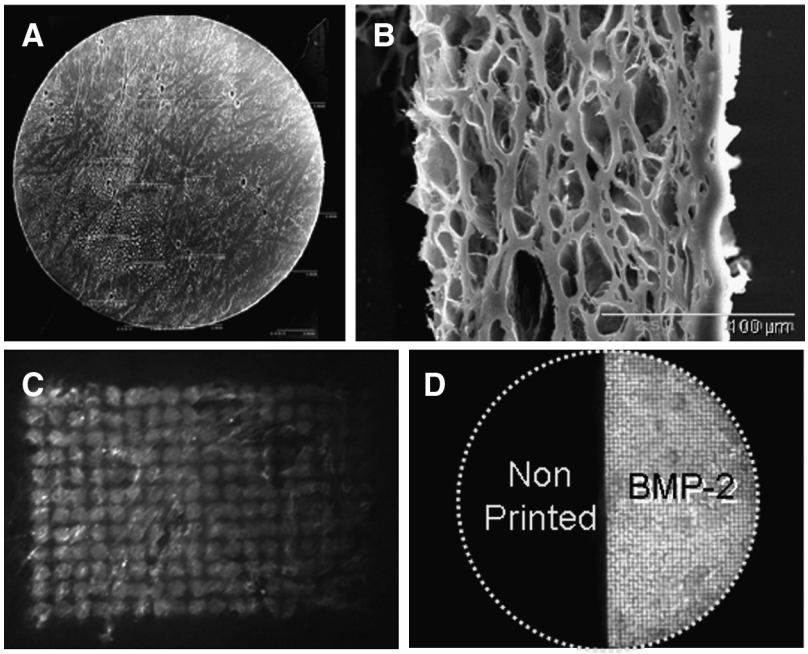

FIG. 2. DermaMatrix as a three-dimensional printing substrate. (**A**) Tiled scanning electron micrograph of 5 mm DermaMatrix disk. (**B**) Scanning electron micrograph of DermaMatrix cross section. Right side represents epidermal layer. (**C**) Fluorescent image of Cy5-bone morphogenetic protein-2 (BMP-2) printed in a gradient upon DermaMatrix. (**D**) Fluorescent image of Cy5-BMP-2 printed on half of 5 mm DermaMatrix disk.

the notch placement, the area of bone formation in either the BMP-2-treated or opposite notched (untreated or noggin treated) half of the defect was determined by subtracting the measured radiographic defect area from the geometric defect area (9.8125 mm^2). Mean measurements of bone area were compared between BMP-2-treated sides and the sides without BMP treatment using ANOVA followed by a least significant differences multiple comparisons test (SYSTAT, v9.0). Following radiographic analysis, skulls were decalcified in 10% ethylenediaminetetraacetic acid, paraffin embedded, cut into 5-µm-thick sections, and stained with hematoxylin and eosin.

Results

In vitro *experiments*

Scanning electron micrographs of DermaMatrix are shown in Figure 2A and B. We were able to print concentration-modulated gradient patterns of Cy5-BMP-2 on DermaMatrix (Fig. 2C). Cy5-BMP-2 was also printed on the right semicircle of a 5-mm-diameter by 200-µm-thick disk of DermaMatrix (Fig. 2D). The depth of bio-ink penetration into DermaMatrix using Cy5-BMP-2 was determined to be on average of 75 µm (range of 65–80 µm) by measuring the axial travel of the piezoelectic z-stage from bottom-to-top of the 3D image stack using a two-photon point scanning laser scanning microscope (data not shown). Cross-sectional scanning electron microscopy (SEM) imaging of the DermaMatrix demonstrated a closed epidermal surface (right side, Fig. 2B) and an open-pore dermal surface (left side, Fig. 2B). The dermal side was used for the printing surface, the cell seeding surface, and the dura mater interface (printed dermal side was placed against the dura *in vivo*).

Printed growth factor patterns must persist to be considered as valid solid-phase patterns. The binding and persistence of solid-phase BMP-2 and noggin in DermaMatrix (Fig. 3) was determined using our previously developed methodology.[31] BMP-2 bound to DermaMatrix in a dose-

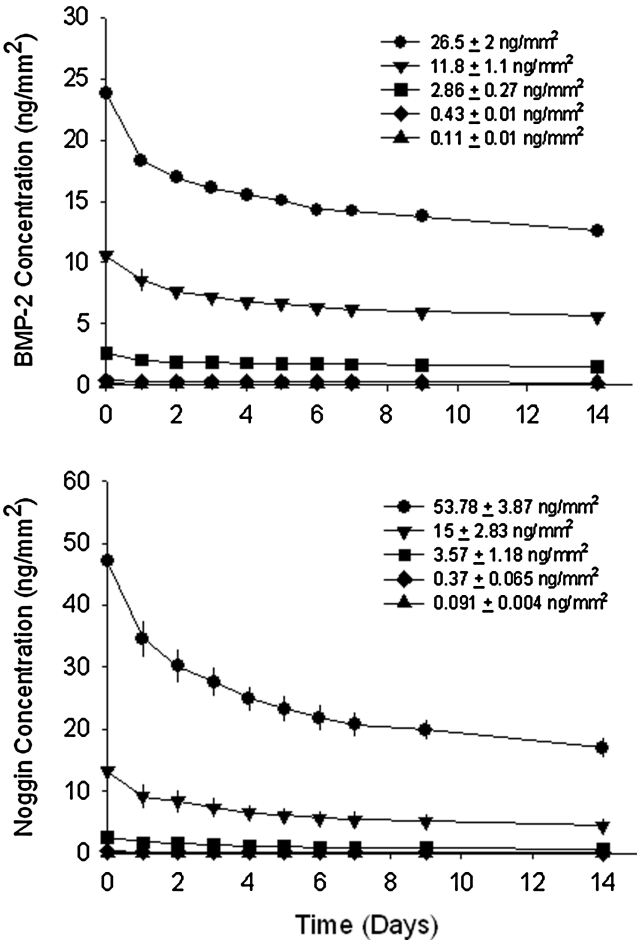

FIG. 3. Binding and retention of printed BMP-2 and noggin on DermaMatrix.

dependent manner for BMP-2 concentrations of 0.11–26.5 ng/mm^2 applied (combined concentration of ^{125}I-labeled and unlabeled BMP-2). Applied surface concentrations in units of ng/mm^2 were calculated as previously described.[27]

Following PBS rinses to remove unbound BMP-2, an average of 90% of printed BMP-2 remained bound across all printed concentrations (time zero on upper graph of Fig. 3). After 24 h of incubation in medium at 37°C, an average of 78.7% BMP-2 remained across all concentrations and subsequent BMP-2 released at a slower rate over the remaining 14 days of study such that ~70% of bound BMP-2 remained.

Noggin also bound to DermaMatrix in a dose-dependent manner for noggin concentrations applied between 0.091 and 53.78 ng/mm^2 (combined concentration of ^{125}I-labeled and unlabeled noggin). Following PBS rinses to remove unbound noggin, an average of 83% of printed noggin remained bound across all printed concentrations (time zero on lower graph of Fig. 3). After 24 h of incubation in medium at 37°C, an average of 69% noggin remained across all concentrations, after which subsequent noggin released at a slower rate over the remaining 14 days of study such that ~50% of bound noggin remained. All printed samples of DermaMatrix used for subsequent *in vitro* and *in vivo* experiments were therefore used only after a minimum of 2 days in PBS.

Spatial control of osteoblastic differentiation of C2C12 cells seeded upon BMP-2-printed patterns of DermaMatrix was demonstrated using ALP staining (Fig. 4). Increasing concentrations of BMP-2 bio-inks (10, 50, or 200 μg/mL BMP-2, 12 OPs each) were printed on the right side of each DermaMatrix scaffold disk, whereas the left sides of the scaffolds represented NP controls (Fig. 4A–C). ALP staining increased with increased amounts of bound BMP-2 (3.73, 18.65, and 74.6 ng total mass of BMP-2 per semicircular pattern). An increase in sporadic staining off pattern was observed as BMP-2 concentration increased, especially evident for the 200 μg/mL dose. This loss of spatial control at high doses suggests spillover effects, presumably caused by desorption of BMP-2 from printed pattern and readsorption off pattern.

To improve spatial control of differentiation, subsequent experiments involved printing one half of each DermaMatrix disk with BMP-2 (200 μg/mL) and printing the opposite

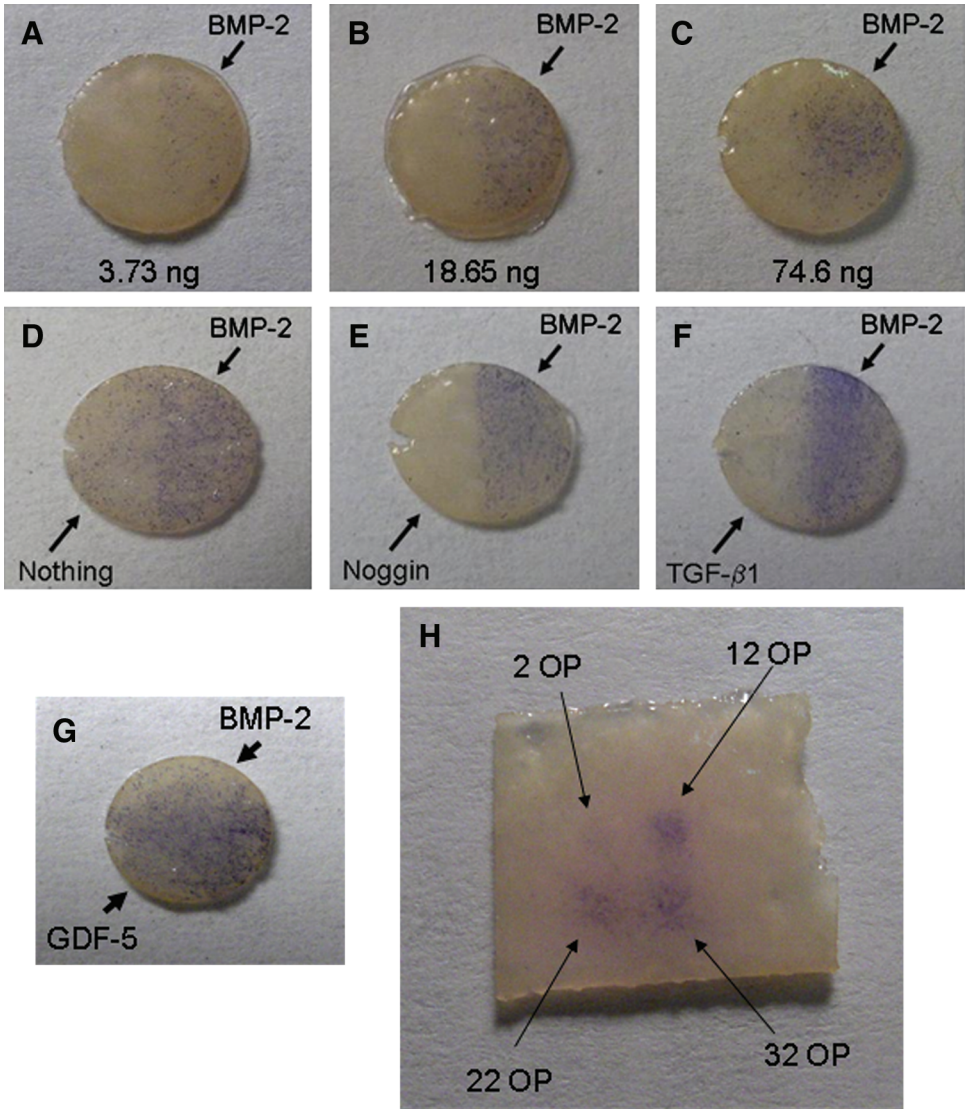

FIG. 4. BMP-2 printed on DermaMatrix stimulates osteogenic cell differentiation in C2C12 cells. All DermaMatrix pieces had right and left semicircular halves printed independently as labeled. Alkaline phosphatase (ALP) staining (blue) shows increased ALP expression with increased doses of BMP-2 (**A–C**). Comparison of different protein combinations showed that noggin was more capable of inhibiting undesired ALP staining (on the left side of the implants) compared with unprinted or transforming growth factor-β1 (TGF-β1)-printed DermaMatrix (**D–F**). Control stimulatory growth factor (GDF-5) showed increased ALP activity on the left side of the DermaMatrix (side not printed with BMP-2) (**G**). C2C12 cells seeded randomly onto DermaMatrix show an ALP staining dose response to printed BMP-2 (**H**). Higher concentrations of BMP-2 are achieved by increasing the number of bio-ink overprints (OPs). Images are representative of at least three separate experiments. Color images available online at www.liebertonline.com/ten.

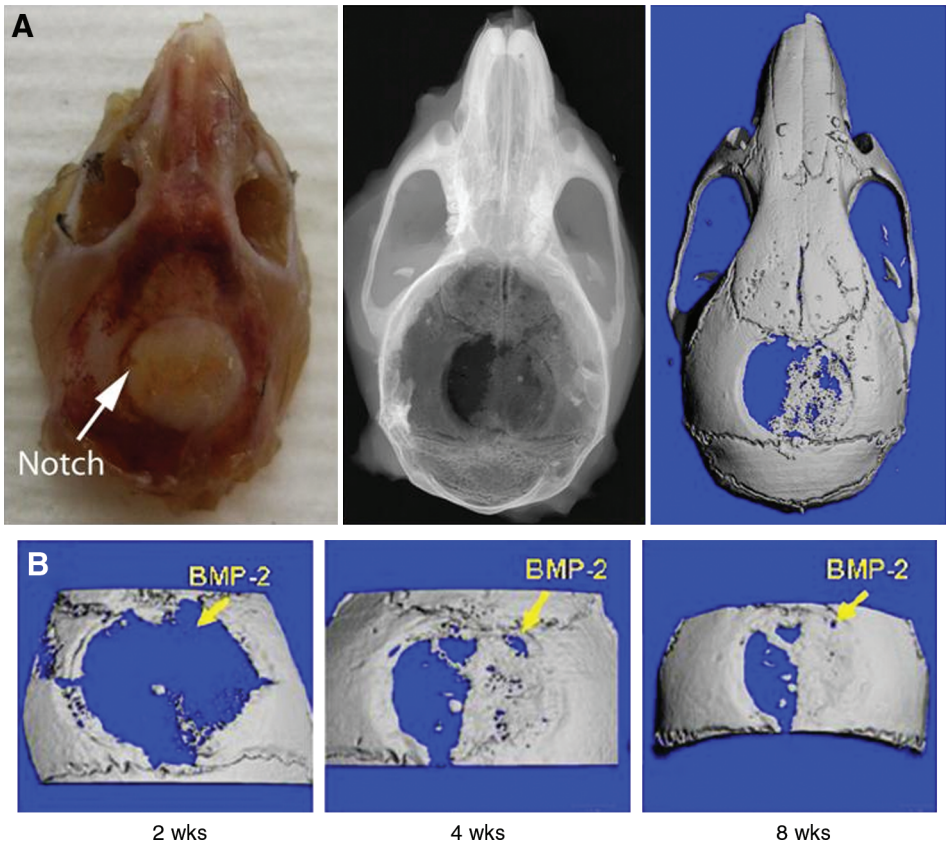

FIG. 5. Applying BMP-2-printed DermaMatrix constructs in a critical-sized mouse defect model to spatially control bone formation. **A**) Photograph (left), radiograph (center), and 3D CT (right) of implanted skull 2 weeks postoperative. **B**) 3D CT reconstructions of one animal 2 weeks, 4 weeks, and 8 weeks postoperative. Color images available online at www.liebertonline.com/ten.

half with modifiers of BMP-2 stimulation, including noggin (50 μg/mL), transforming growth factor β1 (TGF-β1; 100 μg/mL), or GDF-5 (100 μg/mL; Fig. 4E–G). The 200 μg/mL dose of BMP-2 exhibited spillover effects resulting in ALP-positive staining on the NP side of each implant (Fig. 4D). This undesired ALP activity was efficiently inhibited by printing noggin opposite to BMP-2 (Fig. 4E). TGF-β1 was not an efficient inhibitor and appeared to enhance ALP expression on the BMP-2 side (Fig. 4F). As an additional control, GDF-5, which promotes ALP activity, was printed on the side opposite of BMP-2 (Fig. 4G). This resulted in a complete filling of the disk surface with ALP-positive cells. Figure 4H shows a 2×2 printed array of BMP-2 on DermaMatrix using increasing OP of 50 μg/mL BMP-2 bio-ink.

In vivo *experiments*

To demonstrate the translational potential of our printing methodology, BMP-2- and noggin-printed constructs were implanted *in vivo.* Printed BMP-2 patterns were oriented on either the right or the left side of the defect mouse calvarial defects. Constructs printed with BMP-2 showed evidence of bone formation as early as 2 weeks postoperatively (Fig. 5A). After locating the notch that was made in the DermaMatrix opposite to the BMP-2 pattern, we identified that bone preferentially formed in registration with the printed BMP-2 pattern. Further, the shape of the bone that formed by 4 weeks postoperatively was similar to the shape found 8 weeks after implantation (Fig. 5B), indicating the temporal persistence of spatial control.

Some animals received bilateral semicircular patterns of the following combination pairs: (1) DermaMatrix NP on both

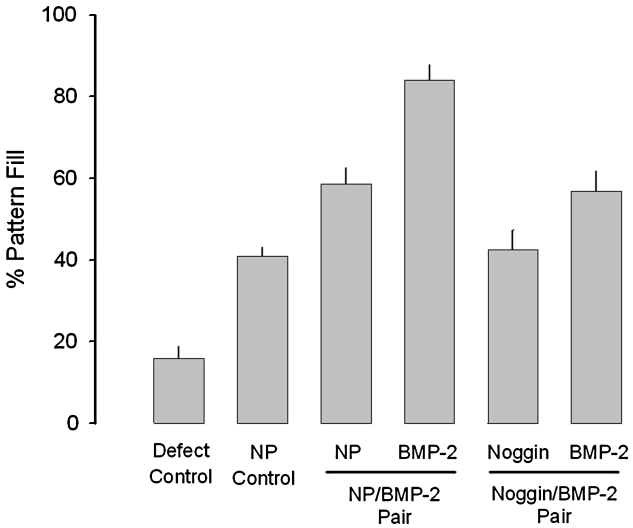

FIG. 6. The effect of various applied patterns on bone fill in register to applied pattern. Treatment groups were defects with unfilled (Defect Control, $n=20$), paired nonprinted (NP) DermaMatrix disks (NP Control, $n=10$), NP control ($n=20$) adjacent to BMP-2 (100 μg/mL BMP-2, 12 OPs, $n=20$) pairs, and noggin (100 μg/mL BMP-2, 12 OPs, $n=18$) adjacent to BMP-2 ($n=18$). Animals were sacrificed after 4 weeks and evaluated by radiography. Data are presented as mean percentage of pattern fill ± standard error of the mean.

semicircular sides; (2) DermaMatrix printed on one semicircular side with BMP-2 (37.5 ng) and the other NP; (3) DermaMatrix printed on one semicircular side with BMP-2 (37.5 ng) and the other printed with noggin (37.5 ng); and (4) no DermaMatrix construct (defect left unfilled). For BMP-2/NP- and BMP-2/noggin-paired DermaMatrix disks, half of the animals received the BMP-2 on the right side of the defect and the other half on the left side. Animals were euthanized at 4 weeks and the percentage of pattern fill measured by radiography was determined as follows: 100×2D bone area within applied semicircular pattern/total area of semicircular pattern (total area = 9.8125 mm^2), where complete bone formation in register to pattern is represented as 100% pattern fill (Fig. 6). There was no effect due to the side of the calvarial defect in which BMP-2 or noggin was placed ($p = 0.717$); therefore, side orientation was not separated for further analysis. Limited healing of the defect occurred when the defect remained completely untreated (15.87% ± 3.1% pattern fill, $n = 20$ semicircular patterns; Fig. 6), primarily associated with bone fill occurring from the calvarial defect perimeter. The application of unprinted DermaMatrix disks resulted in a significant increase in bone fill (40.9% ± 2.2% pattern fill, $n = 10$) over the untreated defect control ($p < 0.0001$), representing an approximate 2.6-fold increase in bone formation. For DermaMatrix disk with paired BMP-2 and NP patterns, BMP-2 patterns resulted in a pattern fill of 84.1% ± 3.7% ($n = 20$) compared with the contralateral unprinted control of 58.7% ± 3.8% ($n = 20$), representing an increase in bone formation of approximately 1.43-fold ($p = 0.001$). Interestingly, when NP patterns were compared between NP/NP and

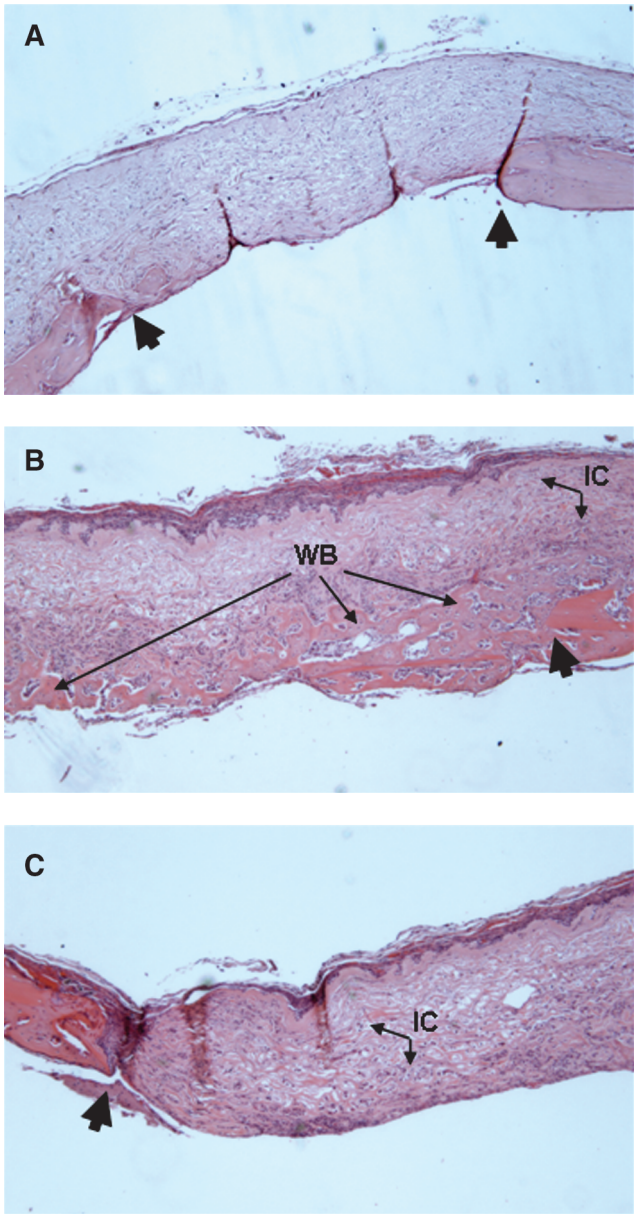

FIG. 7. Hematoxylin and eosin (H&E) histological staining for representative unprinted DermaMatrix (**A**) and DermaMatrix printed half with 100 µg/mL BMP-2, 12 OPs (**B**) and half left unprinted (**C**). Large black arrows denote calvarial defect perimeter. IC, invading undefined cells; WB, woven bone (magnification, ×50).

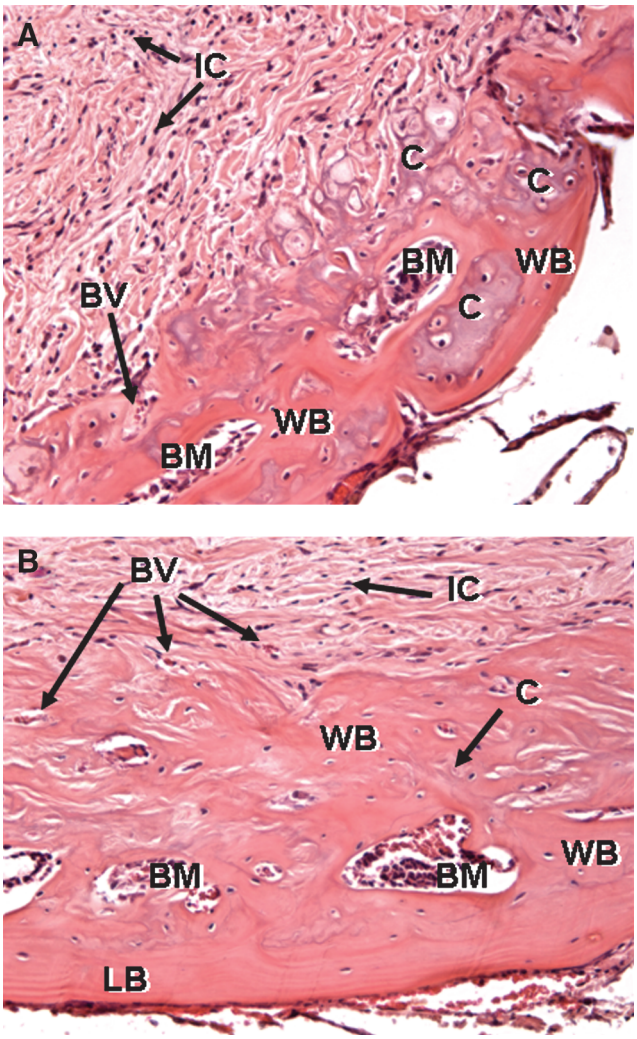

FIG. 8. Higher magnification of H&E histological staining for representative DermaMatrix printed disks at 4 weeks (**A**) and 8 weeks (**B**) using 100 µg/mL BMP-2, 12 OPs. IC, invading undefined cells; WB, woven bone; BM, bone marrow space; BV, blood vessel; C, endochondral bone; LB, lamellar bone (magnification, ×200).

NP/BMP-2 pairs, there was a significant increase in pattern fill for NP patterns adjacent to BMP-2 patterns representing an approximate 1.44-fold increase ($p = 0.007$). These results likely represent spillover from BMP-2 patterns to neighboring contralateral non-BMP-2 patterns. When noggin/BMP-2-paired DermaMatrix disks were applied, noggin ($42.5\% \pm 4.89\%$, $n = 18$) eliminated the observed spillover from adjacent BMP-2 patterns such that the percentage of pattern fill was equivalent between NP ($40.9\% \pm 2.2\%$) from NP/NP-paired DermaMatrix disks ($p = 0.8$). However, noggin patterns induced a significant reduction in pattern fill in neighboring BMP-2 patterns ($56.9\% \pm 5.01\%$, $n = 18$) compared with NP/BMP-2 pairs ($84.1\% \pm 3.7\%$, $n = 20$; $p < 0.001$). These results likely represent spillover from noggin patterns to neighboring contralateral nonnoggin patterns. Nonetheless, BMP-2 patterns from noggin/BMP-2 pairs resulted in greater pattern fill compared with NP from NP/NP pairs ($p < 0.017$). Overall, bone formation occurring within the defect was in register to BMP-2 patterns delivered.

Histological analysis was performed on samples at 2, 4, or 8 weeks postoperatively. Hematoxylin and eosin-stained sections show that DermaMatrix alone does not result in widespread bone formation (Fig. 7A). Bone formation was spatially restricted to the BMP-2-printed half of the construct (Fig. 7B) with essentially no bone formation in the unprinted half (Fig. 7C). Importantly, not only was bone formation restricted to the printed BMP-2 pattern in the x, y plane, but also along the z axis.

High-magnification histological analysis demonstrated that bone formation in the BMP-2-printed region formed through endochondral bone formation. At 2 weeks (Fig. 8A), cartilagenous pockets within BMP-2 patterns are evident with some woven bone surrounding them. Extensive cellular invasion occurred throughout the DermaMatrix. At 8 weeks (Fig. 8B), woven bone formed within the DermaMatrix scaffold essentially restricted to the BMP-2 pattern. Of special note is that the ventral aspect of the DermaMatrix construct (Fig. 8B) shows remodeling of the woven bone into more mature lamellar bone.

Discussion

We previously demonstrated that inkjet-based bioprinting can be used to spatially pattern growth factors on ECM-derived protein-based substrates, such as fibrin. Also, these 2D patterns persist and direct cell behavioral responses *in vitro* in register to the patterns.[27,30,31] We used an inkjetting approach to pattern growth factors for the following reasons: (1) deposited concentrations of growth factors can be easily modulated by overprinting individual locations with dilute bio-inks[27,28]; (2) inkjetting is completely programmable, so custom templates are not required to create specific patterns, and therefore, experimental turn-around times are relatively quick; (3) an almost endless variety and combinations of bio-inks can be deposited with inkjets; (4) inkjetting is scalable; (5) printing is noncontact; and (6) as now described in this article, 2D inkjet patterning is directly translatable to manufacturing 3D growth factor/scaffold constructs. A possible disadvantage of using inkjetting is that it has lower resolution than soft lithographic, photolithographic, or microfluidic protein patterning techniques.[38,39] However, we have shown that the resolution achievable with inkjet printing is sufficient to produce a patterned cellular biological response.

Here we have demonstrated the extension of 2D bioprinting to 3D by bioprinting BMP-2 onto DermaMatrix scaffolds to form 3D constructs by absorption into and binding of BMP-2 bio-ink within scaffolds. We have also demonstrated that such 3D patterned BMP-2 spatially controlled osteoblast formation *in vitro*. Osteoblast differentiation, evidenced by ALP staining, occurred in register to printed BMP-2 patterns. Spillover of ALP staining from BMP-2 patterns could be minimized through the use of a contralateral copatterned delivery of noggin, a BMP-2 inhibitor. Spillover effects of BMP-2 and noggin off their respective printed patterns were also observed in the cells contained off the constructs on the underlying cell culture well surfaces, with a decrease in overall ALP staining observed for noggin and an increase in overall ALP staining observed for BMP-2. Whether this inhibition of ALP activity reflects desorbed bio-inks diffusing off pattern to impact these cells directly or whether this represents *de novo* signaling from cells on printed patterns to cells off pattern remains unclear and the subject for future experiments. Future experiments will consider improving the registration fidelity between patterned bio-inks and subsequent biological responses by improving bio-ink binding retention. Alternative options include using engineered bio-inks designed for improved binding, chemically crosslinking bio-inks to substrates, and altering substrate chemistry to improve binding of bio-inks.

Similarly, *in vivo* results demonstrated a direct translation of *in vitro* findings to an *in vivo* model in which bone formed in register to printed BMP-2 and noggin as evidenced by radiographic, microcomputed tomography, and histological data. To our knowledge this is the first report where a "treatment group" can be compared with a control group for tissue formation within the same construct. The ability to spatially control tissue formation within a construct will allow more precise *in vivo* experimentation consisting of internal controls.

Further, using DermaMatrix printed with 100 μg/mL BMP-2 bio-ink resulted in a total delivered BMP-2 dose of 29.8 ng per semicircular pattern. This dose represents a total of 37.3 ng applied. With ~80% remaining within the scaffold for delivery *in vivo* following the preincubation to remove unbound BMP-2, the delivered dose was far below typical threshold BMP-2 dosages.[40] We are aware of only one other report of similar BMP-2 dosing in a related calvarial model,[41] which, however, used traditional PLGA scaffolds without intraconstruct spatial control.

We have previously demonstrated that the bioactivity of solid-phase growth factors can increase relative to liquid-phase delivery,[28] including BMP-2.[31] Immobilization of both BMP-2 and noggin are known to impact their respective biological activities.[33,42–45] For example, increased bioactivity of BMP-2 may be attributable in part to increased resistance to proteolytic degradation, restricting diffusion, and/or synergistic interaction between BMP-2 receptors and integrins.[33,46]

DermaMatrix did not represent a completely neutral scaffold for this particular study as evidenced by DermaMatrix NP controls exhibiting a higher percentage of bone fill than untreated defect controls. This is likely due to the osteoconductive nature of DermaMatrix as well as the pos-

sibility of osteogenic properties due to residual growth factors not removed during the DermaMatrix manufacturing process. Although bioprinting is compatible with many other scaffold materials, DermaMatrix is a viable option for clinical application. It has been previously shown to have low immunogenicity[47] and to vascularize following implantation in humans.[48] In this study, DermaMatrix was shown to (1) support cell growth *in vitro*, (2) cellularize and support neovascularization after implantation *in vivo*, and (3) allow for bone formation. Further, printed DermaMatrix constructs can be stored dry, which is compatible with surgical logistics.

Beyond biopatterning's use for basic biological studies, this technology shows promise for direct translation to clinical therapies. Inkjetting enables precise, repeatable dosing and efficient use of expensive growth factors. As bone tissue engineering seeks to regenerate diseased or damaged bone, it is important to spatially restrict regeneration to avoid undesired stimulation of or impingement upon surrounding nonbone tissues. The results reported here suggest that bioprinting of BMP-2, alone or in combination with noggin, may be an effective option to spatially control clinically relevant tissue boundary formation.[49] For example, craniosynostosis is the premature fusion of one of more of the calvarial sutures, the narrow regions of nonbone tissue between the bones of the skull. Sutures normally function in part to allow normal brain growth and to transmit mechanical forces generated by mastication or trauma.[50,51] Craniosynostosis represents a failure to form a functional boundary between bones.[52] Our biopatterning method represents an alternative approach to augment surgical intervention[53] for reestablishing these suture boundaries for the purpose of reestablishing normal brain growth vectors and intracranial volume.

Another application for biopatterning technologies is to explore the various patterning cues that will help to establish spatially defined boundaries between tissues within multitissue anatomical units, such as muscle-to-bone or muscle-to-tendon-to-bone. Our prior demonstration of selectively driving a stem cell population to muscle–bone boundaries *in vitro*[31] represented a first-order feasibility of spatially controlling muscle-to-bone attachments, which are anatomically relevant in diverse tissues such as the tibia,[54] the maxilla and mandible,[55,56] and the anterior deltoid.[57]

The bioprinting methodology presented here demonstrated patterning in 200-μm (average)-thick scaffold sheets. Larger or more complex 3D structures could be formed using our method of layered scaffold assembly[28,58] in which each bioprinted layer would be individually patterned prior to assembly. Further, multimaterial structures could be created using different scaffold materials in different layers. Such constructs could also be used in conjunction with a cell therapy.

Acknowledgments

This work was supported partially by the Air Force Multidisciplinary University Research Initiative (F49620-02-1-0359), National Institute for Occupational Safety and Health/Centers for Disease Control and Prevention (200-2002-00528), the National Science Foundation (grants CTS-0210238 and DMI-9800565), the National Institutes of Health (grants 1 R01 EB004343, to P.G.C.; 1 R01 DE019430, to G.M.C.), the Pennsylvania Infrastructure Technology Alliance from the Pennsylvania Department of Community and Economic Development, the Health Resources and Services Administration (grant 1C76 HF 00381-01), the National Tissue Engineering Center, the Department of Defense, the Scaife Foundation, the Philip and Marsha Dowd Engineering Seed Fund, the Plastic Surgery Education Foundation, the Cleft Palate Foundation, and the American Society of Maxillofacial Surgeons. The authors thank Lawrence Schultz for technical support in printing, Dr. Joseph Suhan for processing SEM samples, Dr. James Fitzpatrick for support in fluorescent imaging, and Synthes for donating inkjets DermaMatrix.

Disclosure Statement

No competing financial interests exist. DermaMatrix is the registered trademark of Synthes.

References

1. Tabata, T., and Takei, Y. Morphogens, their identification and regulation. Development **131,** 703, 2004.
2. Gurdon, J.B., and Bourillot, P.Y. Morphogen gradient interpretation. Nature **413,** 797, 2001.
3. Teleman, A.A., Strigini, M., and Cohen, S.M. Shaping morphogen gradients. Cell **105,** 559, 2001.
4. Strigini, M., and Cohen, S.M. Wingless gradient formation in the Drosophila wing. Curr Biol **10,** 293, 2000.
5. Entchev, E.V., and Gonzalez-Gaitan, M.A. Morphogen gradient formation and vesicular trafficking. Traffic **3,** 98, 2002.
6. Podos, S.D., and Ferguson, E.L. Morphogen gradients: new insights from DPP. Trends Genet **15,** 396, 1999.
7. Tickle, C. Morphogen gradients in vertebrate limb development. Semin Cell Dev Biol **10,** 345, 1999.
8. Tickle, C., Summerbell, D., and Wolpert, L. Positional signalling and specification of digits in chick limb morphogenesis. Nature **254,** 199, 1975.
9. Vicker, M.G. Gradient and temporal signal perception in chemotaxis. J Cell Sci **92 (Pt 1),** 1, 1989.
10. Wilkinson, P.C. How do leucocytes perceive chemical gradients? FEMS Microbiol Immunol **2,** 303, 1990.
11. Zachariae, C.O. Chemotactic cytokines and inflammation. Biological properties of the lymphocyte and monocyte chemotactic factors ELCF, MCAF and IL-8. Acta Derm Venereol Suppl (Stockh) **181,** 1, 1993.
12. Einhorn, T.A. Enhancement of fracture-healing. J Bone Joint Surg Am **77,** 940, 1995.
13. Singer, A.J., and Clark, R.A. Cutaneous wound healing. N Engl J Med **341,** 738, 1999.
14. Clark, R.A. Synergistic signaling from extracellular matrix-growth factor complexes. J Invest Dermatol **128,** 1354, 2008.
15. Sahni, A., Odrljin, T., and Francis, C.W. Binding of basic fibroblast growth factor to fibrinogen and fibrin. J Biol Chem **273,** 7554, 1998.
16. Sahni, A., and Francis, C.W. Stimulation of endothelial cell proliferation by FGF-2 in the presence of fibrinogen requires alphavbeta3. Blood **104,** 3635, 2004.
17. Campbell, P.G., and Andress, D.L. Insulin-like growth factor (IGF)-binding protein-5-(201–218) region regulates hydroxyapatite and IGF-I binding. Am J Physiol **273,** E1005, 1997.

18. Campbell, P.G., Durham, S.K., Hayes, J.D., Suwanichkul, A., and Powell, D.R. Insulin-like growth factor-binding protein-3 binds fibrinogen and fibrin. J Biol Chem **274,** 30215, 1999.
19. Sahni, A., Altland, O.D., and Francis, C.W. FGF-2 but not FGF-1 binds fibrin and supports prolonged endothelial cell growth. J Thromb Haemost **1,** 1304, 2003.
20. Gray, A., Dull, T.J., and Ullrich, A. Nucleotide sequence of epidermal growth factor cDNA predicts a 128,000-molecular weight protein precursor. Nature **303,** 722, 1983.
21. Mroczkowski, B., Reich, M., Chen, K., Bell, G.I., and Cohen, S. Recombinant human epidermal growth factor precursor is a glycosylated membrane protein with biological activity. Mol Cell Biol **9,** 2771, 1989.
22. Ferrara, N., and Gerber, H.P. The role of vascular endothelial growth factor in angiogenesis. Acta Haematol **106,** 148, 2001.
23. Botta, M., Manetti, F., and Corelli, F. Fibroblast growth factors and their inhibitors. Curr Pharm Des **6,** 1897, 2000.
24. Lee, S.J. Cytokine delivery and tissue engineering. Yonsei Med J **41,** 704, 2000.
25. Goldring, M.B., and Goldring, S.R. Skeletal tissue response to cytokines. Clin Orthop Relat Res **258,** 245, 1990.
26. Price, J.S., Oyajobi, B.O., and Russell, R.G. The cell biology of bone growth. Eur J Clin Nutr **48 Suppl 1,** S131, 1994.
27. Campbell, P.G., Miller, E.D., Fisher, G.W., Walker, L.M., and Weiss, L.E. Engineered spatial patterns of FGF-2 immobilized on fibrin direct cell organization. Biomaterials **26,** 6762, 2005.
28. Campbell, P.G., and Weiss, L.E. Tissue engineering with the aid of inkjet printers. Expert Opin Biol Ther **7,** 1123, 2007.
29. Weiss, L., Amon, C., Finger, S., Miller, E., Romero, D., Verdinnli, I., Walker, L.W., and Campbell, P.G. Bayesian computer-aided experimental design of heterogenous scaffolds for tissue engineering. Comput Aided Des **37,** 1127, 2005.
30. Miller, E.D., Fisher, G.W., Weiss, L.E., Walker, L.M., and Campbell, P.G. Dose-dependent cell growth in response to concentration modulated patterns of FGF-2 printed on fibrin. Biomaterials **27,** 2213, 2006.
31. Phillippi, J.A., Miller, E., Weiss, L., Huard, J., Waggoner, A., and Campbell, P. Microenvironments engineered by inkjet bioprinting spatially direct adult stem cells toward muscle- and bone-like subpopulations. Stem Cells **26,** 127, 2008.
32. Ruppert, R., Hoffmann, E., and Sebald, W. Human bone morphogenetic protein 2 contains a heparin-binding site which modifies its biological activity. Eur J Biochem **237,** 295, 1996.
33. Rider, C.C. Heparin/heparan sulphate binding in the TGF-beta cytokine superfamily. Biochem Soc Trans **34,** 458, 2006.
34. Miller, E.D., Phillippi, J.A., Fisher, G.W., Campbell, P.G., Walker, L.M., and Weiss, L.E. Inkjet printing of growth factor concentration gradients and combinatorial arrays immobilized on biologically-relevant substrates. Comb Chem High Throughput Screen **12,** 604, 2009.
35. Canalis, E., Economides, A.N., and Gazzerro, E. Bone morphogenetic proteins, their antagonists, and the skeleton. Endocr Rev **24,** 218, 2003.
36. Mujumdar, R.B., Ernst, L.A., Mujumdar, S.R., Lewis, C.J., and Waggoner, A.S. Cyanine dye labeling reagents: sulfoindocyanine succinimidyl esters. Bioconjug Chem **4,** 105, 1993.
37. Campbell, P.G., Skaar, T.C., Vega, J.R., and Baumrucker, C.R. Secretion of insulin-like growth factor-I (IGF-I) and IGF-binding proteins from bovine mammary tissue *in vitro*. J Endocrinol **128,** 219, 1991.
38. Ito, Y., Hayashi, M., and Imanishi, Y. Gradient micropattern immobilization of heparin and its interaction with cells. J Biomater Sci Polym Ed **12,** 367, 2001.
39. Whitesides, G.M., Ostuni, E., Takayama, S., Jiang, X., and Ingber, D.E. Soft lithography in biology and biochemistry. Annu Rev Biomed Eng **3,** 335, 2001.
40. Cowan, C.M., Soo, C., Ting, K., and Wu, B. Evolving concepts in bone tissue engineering. Curr Top Dev Biol **66,** 239, 2005.
41. Cowan, C.M., Aghaloo, T., Chou, Y.F., Walder, B., Zhang, X., Soo, C., Ting, K., and Wu, B. MicroCT evaluation of three-dimensional mineralization in response to BMP-2 doses *in vitro* and in critical sized rat calvarial defects. Tissue Eng **13,** 501, 2007.
42. Jiao, X., Billings, P.C., O'Connell, M.P., Kaplan, F.S., Shore, E.M., and Glaser, D.L. Heparan sulfate proteoglycans (HSPGs) modulate BMP2 osteogenic bioactivity in C2C12 cells. J Biol Chem **282,** 1080, 2007.
43. Saito, K., Konishi, I., Nishiguchi, M., Hoshino, T., and Fujiwara, T. Amelogenin binds to both heparan sulfate and bone morphogenetic protein 2 and pharmacologically suppresses the effect of noggin. Bone **43,** 371, 2008.
44. Fisher, M.C., Li, Y., Seghatoleslami, M.R., Dealy, C.N., and Kosher, R.A. Heparan sulfate proteoglycans including syndecan-3 modulate BMP activity during limb cartilage differentiation. Matrix Biol **25,** 27, 2006.
45. Paine-Saunders, S., Viviano, B.L., Economides, A.N., and Saunders, S. Heparan sulfate proteoglycans retain Noggin at the cell surface: a potential mechanism for shaping bone morphogenetic protein gradients. J Biol Chem **277,** 2089, 2002.
46. Jadlowiec, J.A., Zhang, X., Li, J., Campbell, P.G., and Sfeir, C. Extracellular matrix-mediated signaling by dentin phosphophoryn involves activation of the Smad pathway independent of bone morphogenetic protein. J Biol Chem **281,** 5341, 2006.
47. Gordley, K., Cole, P., Hicks, J., and Hollier, L. A comparative, long term assessment of soft tissue substitutes: AlloDerm, Enduragen, and Dermamatrix. J Plast Reconstr Aesthet Surg **62,** 849, 2009.
48. Becker, S., Saint-Cyr, M., Wong, C., Dauwe, P., Nagarkar, P., Thornton, J.F., and Peng, Y. AlloDerm versus DermaMatrix in immediate expander-based breast reconstruction: a preliminary comparison of complication profiles and material compliance. Plast Reconstr Surg **123,** 1; discussion 107, 2009.
49. Dahmann, C., and Basler, K. Compartment boundaries: at the edge of development. Trends Genet **15,** 320, 1999.
50. Opperman, L.A. Cranial sutures as intramembranous bone growth sites. Dev Dyn **219,** 472, 2000.
51. Herring, S.W. Mechanical influences on suture development and patency. Front Oral Biol **12,** 41, 2008.
52. Merrill, A.E., Bochukova, E.G., Brugger, S.M., Ishii, M., Pilz, D.T., Wall, S.A., Lyons, K.M., Wilkie, A.O.M., and Maxon, R.E. Cell mixing at a neural crest-mesoderm boundary and deficient ephrin-Eph signaling in the pathogenesis of craniosynostosis. Hum Mol Genet **15,** 1319, 2006.
53. Persing, J.A., Edgerton, M.A., and Jane, J.A. Surgical treatment of craniosynostosis. In: Persing, J.A., Edgerton, M.A., and Jane, J.A., eds. Scientific Foundations and Surgical Treatment of Craniosysnostosis. Baltimore: William and Wilkins, 1989, pp. 87–95.
54. Benjamin, M., Kumai, T., Milz, S., Boszczyk, B.M., Boszczyk, A.A., and Ralphs, J.R. The skeletal attachment of tendons—

tendon "entheses." Comp Biochem Physiol A Mol Integr Physiol **133,** 931, 2002.
55. Sinsel, N.K., and Guelinckx, P.J. Effect of unilateral partial facial paralysis on periosteal growth at the muscle-bone interface of facial muscles and facial bones. Plast Reconstr Surg **111,** 1432; discussion 44, 2003.
56. Chong, D.A., and Evans, C.A. Histologic study of the attachment of muscles to the rat mandible. Arch Oral Biol **27,** 519, 1982.
57. Kumar, V.P., Satku, K., Liu, J., and Shen, Y. The anatomy of the anterior origin of the deltoid. J Bone Joint Surg Br **79,** 680, 1997.
58. Weiss, L.E., and Szem, J. Assembled scaffolds for three dimensional cell culture and tissue regeneration. U.S. Patent 6143293, 2000.

Address correspondence to:
Gregory M. Cooper, Ph.D.
Departments of Surgery, Oral Biology, and Bioengineering
University of Pittsburgh
3510 Rangos Research Center
Children's Hospital of Pittsburgh
One Children's Hospital Drive
4401 Penn Ave.
Pittsburgh, PA 15224

E-mail: greg.cooper@chp.edu

Received: September 29, 2009
Accepted: December 15, 2009
Online Publication Date: February 9, 2010